

Stability of self-gravitating discs under irradiation

W. K. M. Rice^{1*}, P. J. Armitage^{2,3}, G.R. Mamatsashvili^{1,4}, G. Lodato⁵ and C. J. Clarke⁶

¹*Scottish Universities Physics Alliance (SUPA), Institute for Astronomy, University of Edinburgh, Blackford Hill, Edinburgh EH9 3HJ*

²*JILA, 440 UCB, University of Colorado, Boulder, CO 80309-0440, USA*

³*Department of Astrophysical and Planetary Sciences, University of Colorado, Boulder, USA*

⁴*Georgian National Astrophysical Observatory, Il. Chavchavadze State University, 2a Kazbegi Ave., Tbilisi 0160, Georgia*

⁵*Università degli Studi di Milano, Dipartimento di Fisica, via Celoria 16, I-20133 Milano, Italy*

⁶*Institute of Astronomy, Madingley Road, Cambridge, CB3 0HA, UK*

8 August 2011

ABSTRACT

Self-gravity becomes competitive as an angular momentum transport process in accretion discs at large radii, where the temperature is low enough that external irradiation likely contributes to the thermal balance. Irradiation is known to weaken the strength of disc self-gravity, and can suppress it entirely if the disc is maintained above the threshold for linear instability. However, its impact on the susceptibility of the disc to fragmentation is less clear. We use two-dimensional numerical simulations to investigate the evolution of self-gravitating discs as a function of the local cooling time and strength of irradiation. In the regime where the disc does not fragment, we show that local thermal equilibrium continues to determine the stress - which can be represented as an effective viscous α - out to very long cooling times, $\tau_c = 240\Omega^{-1}$. In this regime, it is also found that the power spectrum of the perturbations is uniquely set by this effective viscous α and not by the cooling rate. Fragmentation occurs for $\tau_c < \beta_{\text{crit}}\Omega^{-1}$, where β_{crit} is a weak function of the level of irradiation. We find that β_{crit} declines by approximately a factor of two, as irradiation is increased from zero up to the level where instability is almost quenched. The numerical results imply that irradiation cannot generally avert fragmentation of self-gravitating discs at large radii; if other angular momentum transport sources are weak mass will build up until self-gravity sets in, and fragmentation will ensue.

Key words: accretion, accretion discs — hydrodynamics — protoplanetary disks — stars: formation — galaxies: active

1 INTRODUCTION

Self-gravity may be important in the cool outer regions of both protostellar and Active Galactic Nuclei (AGN) accretion discs, where the combined effects of pressure and shear cannot stabilize the flow against gravitational instability. The local linear stability of self-gravitating discs is simple (Toomre 1964): it depends upon the parameter,

$$Q \equiv \frac{c_s \kappa}{\pi G \Sigma}, \quad (1)$$

where c_s and Σ are the sound speed and surface density of a low-mass disc ($M_{\text{disc}} \ll M_*$), and κ is the epicyclic frequency which, in a Keplerian disc, is the same as the angular velocity Ω . The non-linear behaviour, however, is complex. A self-gravitating disc can either fragment into bound objects, or attain a “stable” self-gravitating state in which angular momentum transport results in

accretion and energy dissipation. Determining what sets the boundary between these outcomes is important for understanding angular momentum transport (Armitage 2011) and planet formation in protoplanetary disks (Boss 1997), and star formation in discs around AGN (Bonnell & Rice 2008).

Since gravity is a long-range force angular momentum transport via self-gravity could in principle be a non-local process (Balbus & Papaloizou 1999). Global numerical simulations (Lodato & Rice 2004; Cossins, Lodato & Clarke 2009), however, show that disc self-gravity can be approximated surprisingly well using a model in which turbulent heating associated with angular momentum transport is *locally* balanced by radiative losses. The use of this local approximation (Paczynski 1978; Lin & Pringle 1987) greatly simplifies the description of the disc. In a local description, thermal equilibrium implies that the stress, measured via the equivalent Shakura-Sunyaev α parameter (Shakura & Sunyaev 1973), is inversely proportional to the time scale on which the disc can radiate its thermal energy (Gammie 2001). The stability of the disc against fragmentation also depends upon its cool-

* E-mail: wkmr@roe.ac.uk

ing time (Shlosman & Begelman 1987). Writing $t_{\text{cool}} = \beta\Omega^{-1}$, two-dimensional local numerical simulations show that fragmentation of a self-luminous disc (one in which the only source of heat is furnished by accretion) ensues whenever $\beta < \beta_{\text{crit}} \approx 3$ (Gammie 2001, assuming a 2D adiabatic index $\gamma = 2$). This minimum cooling time before fragmentation is equivalent to a maximum $\alpha_{\text{crit}} \approx 0.1$ that a stable self-gravitating disc can sustain (Rice, Lodato & Armitage 2005). Consistent results for the location of the fragmentation boundary are obtained from two-dimensional global simulations, provided that care is taken to avoid prompt fragmentation during the initial growth of instability (Paardekooper, Baruteau & Meru 2011). In three-dimensional global simulations the situation is less clear. There is evidence that such discs are somewhat less stable against fragmentation than their two-dimensional counterparts (Meru & Bate 2011), although a critical cooling time does nonetheless appear to exist (Lodato & Clarke 2011; Rice, Forgan & Armitage 2011). We also note that strong temperature dependence of the opacity can modify the fragmentation boundary substantially (Johnson & Gammie 2003; Cossins, Lodato & Clarke 2010). This work deals exclusively with simpler temperature-independent disc cooling.

Applying these results for self-luminous discs to protostellar and AGN discs, fragmentation is predicted to occur for $r \gtrsim 70 - 100$ au in protostellar discs (Matzner & Levin 2005; Rafikov 2005; Stamatellos, Hubber & Whitworth 2007; Boley 2009; Clarke 2009; Rafikov 2009; Rice, Mayo & Armitage 2010), and at $r \gtrsim 0.06 (M_{\text{BH}}/10^6 M_{\odot})^{1/3}$ pc for AGN (Rafikov 2009; Goodman 2003; Levin 2007). At these large radii, however, the temperature of a self-luminous disc is small enough – about 10 K – that the thermal balance of a real disc in a star forming region or galactic nucleus may often be influenced by external irradiation (or, in the AGN case, by internal heating due to embedded stars). Here, we use numerical simulations to revisit the stability of self-gravitating discs, taking into account that irradiation as well as dissipation of accretion energy may contribute to the thermal balance. Our goal is to determine whether, in an irradiated disc, the fragmentation boundary is determined by a minimum cooling time or by a maximum α . These quantities, which are no longer equivalent in a disc subject to irradiation, are both physically important: β measures the time scale on which overdense clumps can radiate thermal energy and collapse further, while α is related to the amplitude and non-linearity of density perturbations. We also address the question of whether an annulus of the disc, initially assumed to be stabilized against self-gravity by irradiation, is able to viscously respond to an increase in surface density without entering the fragmentation regime. This work expands on earlier work by Cai et al. (2008) in which irradiation from an envelope around a protoplanetary disc was shown to weaken the gravitational instability, and is complementary to the analytic discussion in Kratter & Murray-Clay (2011).

The plan of this paper is as follows. In Section 2 we describe the local (shearing-sheet) simulations that we perform to investigate the evolution of irradiated self-gravitating discs, in Section 3 we discuss the results of these simulations, and in Section 4 we discuss some implications of our results.

2 METHOD

To investigate the evolution of self-gravitating discs in the presence of external irradiation we use the Pencil Code, a finite difference code that uses sixth-order centered spatial derivatives and a third-

order Runge-Kutta time-stepping scheme (see Brandenburg (2003) for details). As in Gammie (2001), we use a “shearing sheet”, or “local”, model in which the disc dynamics is studied in a local Cartesian coordinate frame corotating with the angular velocity, Ω , of the disc at some radius from the central star. In this coordinate frame, the unperturbed differential rotation of the disc manifests itself as a parallel azimuthal flow with a constant velocity shear in the radial direction. We assume Keplerian rotation and hence use a shear parameter of $q = 1.5$ (such that the y -component of the fluid velocity is $u_y = -q\Omega x$). The unperturbed background surface density, Σ_0 , and two-dimensional pressure, P_0 , are assumed to be spatially constant. A Coriolis force is included to take into account the effects of the coordinate frame rotation.

To use the “local” model we need to assume that the disc is cool and hence thin ($H/r \approx c_s/(\Omega r) \ll 1$) and, as in Gammie (2001), we also assume that it is razor-thin. The continuity equation and equations of motion in this model are

$$\begin{aligned} \frac{\partial \Sigma}{\partial t} + \nabla \cdot (\Sigma \mathbf{u}) - q\Omega x \frac{\partial \Sigma}{\partial y} &= 0 \\ \frac{\partial u_x}{\partial t} + (\mathbf{u} \cdot \nabla) u_x - q\Omega x \frac{\partial u_x}{\partial y} &= -\frac{1}{\Sigma} \frac{\partial P}{\partial x} + 2\Omega u_y - \frac{\partial \phi}{\partial x} + f_{vx} \\ \frac{\partial u_y}{\partial t} + (\mathbf{u} \cdot \nabla) u_y - q\Omega x \frac{\partial u_y}{\partial y} &= -\frac{1}{\Sigma} \frac{\partial P}{\partial y} + (q-2)\Omega u_x - \frac{\partial \phi}{\partial y} + f_{vy} \end{aligned} \quad (2)$$

where $\mathbf{u}(u_x, u_y)$ is velocity relative to the background parallel shear flow $\mathbf{u}_0(0, -q\Omega x)$, P is the two-dimensional pressure, Σ is the surface density, ϕ is the gravitational potential of the gas sheet, and $\mathbf{f}_v(f_{vx}, f_{vy})$ is a viscosity term that includes both a kinematic viscosity and a bulk viscosity for resolving shocks. Since this disc is razor-thin, Poisson’s equation becomes

$$\nabla^2 \phi = 4\pi G \Sigma \delta(z). \quad (3)$$

This can be solved by Fourier transforming (using the standard Fast Fourier Transform (FFT) technique) the surface density from the (x, y) plane to the (k_x, k_y) plane giving

$$\phi(k_x, k_y, t) = -\frac{2\pi G \Sigma(k_x, k_y, t)}{k}, \quad (4)$$

where $\phi(k_x, k_y, t)$ and $\Sigma(k_x, k_y, t)$ are the Fourier transforms of the gravitational potential and surface density, and $k = \sqrt{k_x^2 + k_y^2}$. It should be noted that in the shearing sheet approximation, the radial wavenumber, k_x , is no longer constant, but varies with time as $k_x(t) = k_x(0) + q\Omega k_y t$. For a two-dimensional domain of size $L \times L$ with resolution $N \times N$, the only Fourier harmonics that will be present at time t will have wavenumbers $k_y = 2\pi n_y/L$ and $k_x = 2\pi n_x/L + q\Omega t'(2\pi n_y/L)$, where $t' = \text{mod}[t, 1/(q\Omega|n_y|)]$, and integer numbers n_x and n_y lie in the range $-N/2 \leq n_x, n_y \leq N/2$. As in Gammie (2001) we only use wavenumbers that satisfy $k < \pi N/(L\sqrt{2})$ which is the largest circular region in Fourier space that is always available, and ensures that the gravitational force is isotropic on small scales.

The equation of state is essentially the standard

$$P = (\gamma - 1)U, \quad (5)$$

where U is the two-dimensional internal energy per unit volume, and γ is the two-dimensional adiabatic index. We use $\gamma = 1.6$ which can be mapped to a three-dimensional adiabatic index of between ~ 1.6 and 1.9 depending on whether the disc is strongly self-gravitating or not (e.g., Gammie (2001)). For protostellar discs, a smaller value of γ may be more appropriate. However, since the work here is not restricted only to protostellar discs, we have cho-

sen to use $\gamma = 1.6$. Rather than solving for internal energy, the Pencil Code actually solves for the specific entropy, s (see Brandenburg (2003) for details). We use a cooling function similar to that used by Gammie (2001) but modified by the inclusion of a heating term that represents external irradiation. When written in terms of specific entropy, the combined heating and cooling function that is imposed is

$$\Sigma T \frac{\partial s}{\partial t} = -\frac{\Sigma(c_s^2 - c_{so}^2)}{\gamma(\gamma - 1)\tau_c}, \quad (6)$$

where T is the temperature corresponding to a sound speed of c_s and τ_c is constant cooling time, generally written as $\tau_c = \beta\Omega^{-1}$ with β a predefined constant. The sound speed, c_{so} , is an effective minimum sound speed set by the background irradiation and which we generally express in terms of an effective Q_{irr} where

$$Q_{\text{irr}} = \frac{c_{so}\Omega}{\pi G \Sigma_o}. \quad (7)$$

All the simulations presented here consider a rectangular box of size $L_x = L_y = L = 320$ with a resolution of $N \times N$ where $N = 1024$, the same as the “standard” run in Gammie (2001). The sound speed, or pressure, and surface density are initially constant and are set such that $Q_{\text{init}} = 1$. The initial perturbations are introduced through the velocity field which is perturbed from the background flow by a Gaussian noise component with a subsonic amplitude. Each simulation has a prescribed cooling time, β , and an imposed level of external irradiation, Q_{irr} .

3 RESULTS

3.1 Evolution without irradiation

We consider initially simulations with no external irradiation ($Q_{\text{irr}} = 0$) and vary the cooling time (as measured by β) to establish the fragmentation boundary and to investigate the quasi-steady nature of those simulations that don’t fragment. A quasi-steady state is one in which Q settles to an approximately constant value, generally between 1 and 2, and remains at this value for many cooling times. In such a state, the instability is active but the system does not fragment and the instability acts to transport angular momentum. The disc is regarded as having fragmented if very dense clumps form, with densities more than 2 orders of magnitude greater than the average density, and survive for many cooling times. The presence of a bound clump also rapidly heats up the surrounding gas and so the Q value in a simulation that fragments also does not settle to an approximately constant value, but continues to rise. Fig. 1 shows the surface density structure from a simulation that has settled into a quasi-steady state. In this case $\beta = 10$ and $Q_{\text{irr}} = 0$. Fig. 2 shows the variation of Q against time illustrating that after an initial burst phase, Q settles into a quasi-steady state with $Q \sim 1.8$ that persists for many cooling times. Note that the saturated value of Q is almost a factor 2 larger than what is usually found in 3D simulations (e.g. Cossins et al 2009), where $Q \sim 1.1$. This is due to the stabilising effect of the finite disc thickness in 3D simulations (Romeo 1992; Mamatsashvili & Rice 2010), which dilutes the effect of gravity by $\sim (1 + kH)$, where k is the wavenumber of the perturbation. Since for the most unstable modes $k \sim 1/H$, we expect a reduction in the linear stability threshold for Q by approximately a factor 2, as observed. Fig. 3 shows the surface density structure for a simulation, with $\beta = 6$ and $Q_{\text{irr}} = 0$, that has undergone fragmentation.

It can be shown that when a system settles into a quasi-steady

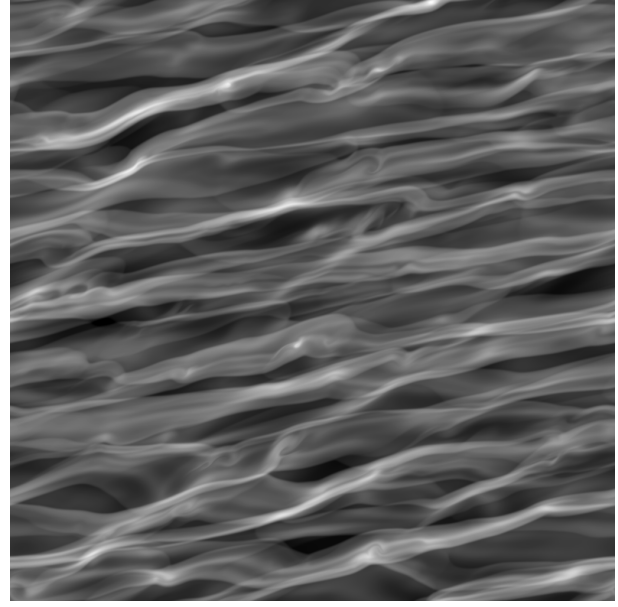


Figure 1. Quasi-steady surface density structure for $\beta = 10$ and $Q_{\text{irr}} = 0$.

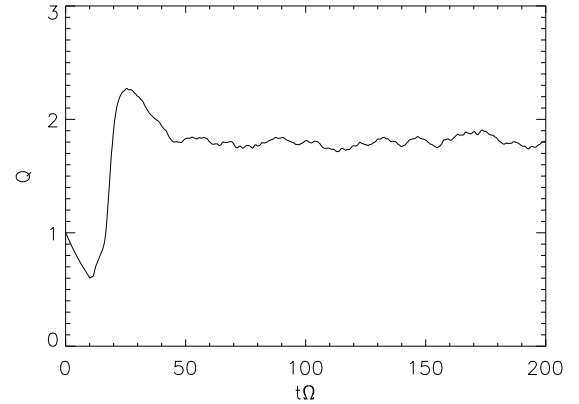


Figure 2. Q profile against time for $\beta = 10$ and $Q_{\text{irr}} = 0$.

state, the shear stress - which we express in terms of an effective α - satisfies the relationship (Pringle 1981; Gammie 2001)

$$\alpha = \frac{4}{9\gamma(\gamma - 1)\tau_c\Omega}. \quad (8)$$

The shear stress can also be determined in each simulation using the Reynolds and gravitational stresses. The average Reynolds stress is

$$\langle H_{xy} \rangle = \langle \Sigma u_x u_y \rangle, \quad (9)$$

where u_x and u_y are, again, the velocity perturbations with respect to the background Keplerian flow. As described in detail in Gammie (2001), the average gravitational shear stress can be determined in the Fourier domain using

$$\langle G_{xy} \rangle = \sum_k \frac{\pi G k_x k_y |\Sigma_k|^2}{|k|^3}, \quad (10)$$

where the sum is over all Fourier components. The effective α is then

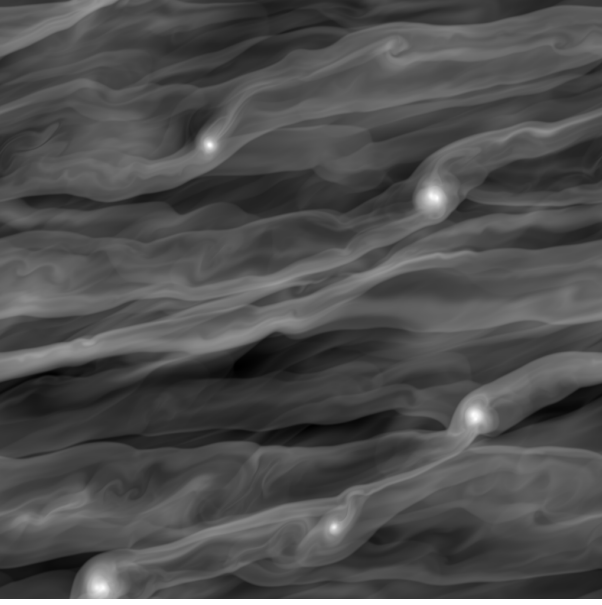


Figure 3. Surface density structure for a simulation, with $\beta = 6$ and $Q_{\text{irr}} = 0$, that has undergone fragmentation.

$$\alpha = \frac{2}{3 \langle \Sigma c_s^2 \rangle} (\langle G_{xy} \rangle + \langle H_{xy} \rangle), \quad (11)$$

which can then be compared with the effective α determined using the imposed cooling time.

We consider a series of simulations with β varying from 4 to 240. We find that fragmentation occurs for $\beta \leq 8$. Gammie (2001) found fragmentation for $\beta \leq 3$ and the reason for the difference is simply that we have considered a different specific heat ratio, γ (Rice, Lodato & Armitage 2005). For each simulation that does not fragment we calculate the effective α from the Reynolds and gravitational stresses using equation (11) and compare it with that expected from the imposed cooling time (e.g., equation (8)). This is illustrated in Fig. 4 in which the measured α values determined using the Reynolds and gravitational stresses are plotted as triangles, while that expected from the imposed cooling are plotted as diamonds. The averaged quantities that are needed to determine the effective α values are written out by the Pencil Code every 100 iterations, corresponding to a time resolution of $\sim \Omega \Delta t = 0.1$, depending on the Courant condition. The measured α values are then determined by averaging over at least a few cooling times (generally 5 or greater, except for the simulations with very long cooling times) starting once the system has settled into a quasi-steady state.

There is a discrepancy between the measured and expected α values, with the mean of the measured values being higher than that expected. The 1σ error bars, however, show that the values are at least consistent. The discrepancy is thought to be due to truncation errors. We have chosen to minimise the kinematic viscosity and as result some energy is lost at the grid scale (Gammie 2001). Figure 4 does, however, show that the maximum stress that can be attained in a quasi-steady system is $\alpha \sim 0.06$, consistent with earlier results (Gammie 2001; Rice, Lodato & Armitage 2005).

3.2 Evolution of irradiated discs

In a quasi-steady state in the absence of external irradiation, the imposed cooling is balanced by heating due to the Reynolds and

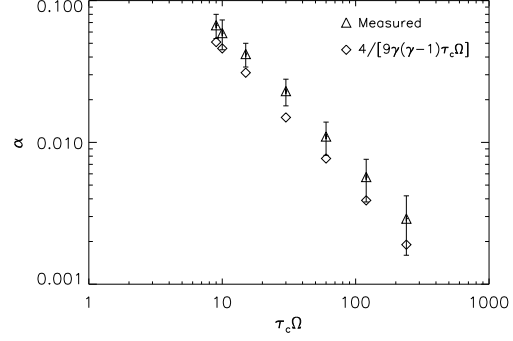


Figure 4. Comparison of the measured effective α values (crosses) determined using equation (11) with that determined from the imposed cooling time (diamonds).

gravitational stresses. To consider the influence of external irradiation, we impose a combined heating and cooling function of the form shown in equation (6). In a quasi-steady state the following should then hold (Gammie 2001; Mamatsashvili & Rice 2009)

$$\frac{3}{2} \Omega \left\langle \Sigma u_x u_y + \frac{1}{4\pi G} \int_{-\infty}^{\infty} \frac{\partial \phi_x}{\partial x} \frac{\partial \phi_y}{\partial y} dz \right\rangle = \frac{3}{2} \Omega (\langle H_{xy} \rangle + \langle G_{xy} \rangle) \quad (12)$$

$$= \frac{\langle \Sigma c_s^2 \rangle - \langle \Sigma \rangle c_{so}^2}{\gamma(\gamma - 1)\tau_c}. \quad (13)$$

Using equation (11) we can therefore show that, with external irradiation included,

$$\alpha \approx \frac{4}{9\gamma(\gamma - 1)\Omega\tau_c} \left(1 - \frac{\langle \Sigma \rangle c_{so}^2}{\langle \Sigma c_s^2 \rangle} \right). \quad (14)$$

If we assume that $\langle \Sigma c_s^2 \rangle \approx \langle \Sigma \rangle \langle c_s \rangle^2$, we can rewrite equation (14) as

$$\alpha \approx \frac{4}{9\gamma(\gamma - 1)\Omega\tau_c} \left(1 - \frac{Q_{\text{irr}}^2}{Q_{\text{sat}}^2} \right), \quad (15)$$

where Q_{sat} is the saturated Q value to which the quasi-steady simulations settle. Since Σ and c_s are probably correlated, the approximation made to go from Equation (14) to Equation (15) may not be accurate, but at least gives us an approximate relationship between α , Q_{irr} and Q_{sat} . The form of equation (15) is also consistent with, and a generalisation of, the expression used by Lin & Pringle (1990) to represent viscosity in a self-gravitating disc.

To establish the influence of external irradiation, we consider various values of β and for each value of β we consider a number of different values of Q_{irr} . Fig. 5 compares the measured α values (determined using the Reynolds and gravitational stresses as described above) with the expected α values determined using equation (14), plotted against Q_{irr} for $\beta = 7$ (top left), $\beta = 8$ (top right), and $\beta = 9$ (bottom). Again, we only include simulations that settle into a quasi-steady, self-gravitating state. The diamonds show the mean of the measured values and the error bars are 1σ errors. The triangles show the expected value determined using Equation (14). Once again, the measured values are higher than those expected but do illustrate, very clearly, that as the level of irradiation increases, the instability weakens - as expected - and the value of α decreases. A quasi-steady α that exceeds the expected maximum of ~ 0.06 is also never measured.

Fig. 6 summarizes our determination of the fragmentation boundary in the (Q_{irr}, β) plane. The plotted contours show lines of

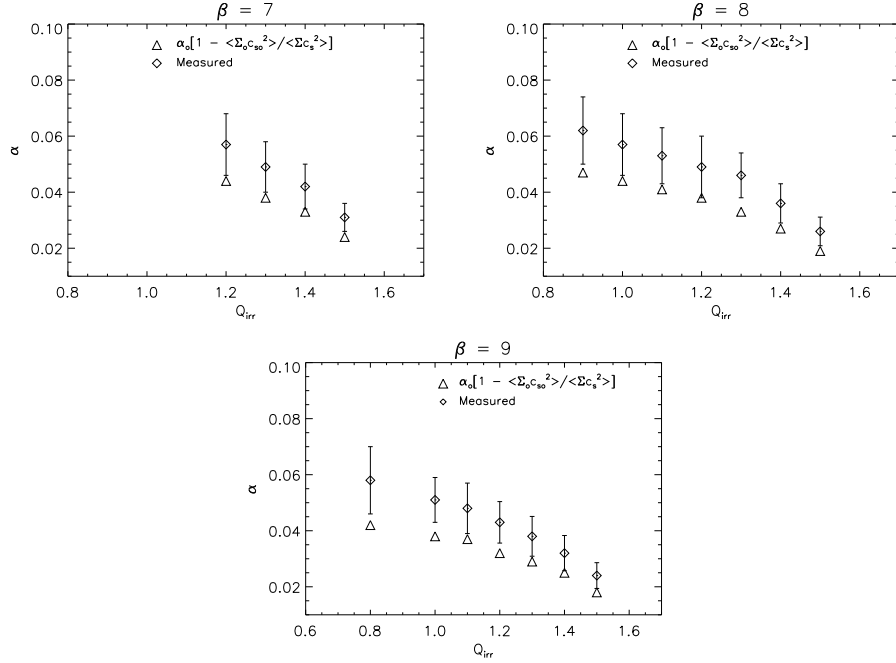


Figure 5. Comparison of measured α values with that determined using the imposed cooling time, plotted against Q_{irr} for $\beta = 7$ (top left), $\beta = 8$ (top right), and $\beta = 9$ (bottom).

constant α , determined using equation (15) with, using Figure 2 as a guide, $Q_{\text{sat}} = 1.9$. Ideally we should be using Equation (14) to set the contours, but we don't really know an appropriate value for $\langle \Sigma c_s^2 \rangle$ or how it might vary with Q_{irr} , so Equation (15) provides a suitable approximation. The contour values, from bottom to top at $Q_{\text{irr}} = 0$, are $\alpha = 0.06, 0.05, 0.04, 0.03, 0.02$ and 0.01 . The symbols in Fig. 6 show all the simulations that have been performed, with the triangles being those that fragmented and the diamonds being those that settled into a quasi-steady state. The number next to each diamond is the measured α value for that simulation.

Fig. 6 illustrates that for every cooling time there is a level of irradiation (Q_{irr}) for which fragmentation does not occur. However, the boundary between fragmentation or a quasi-steady, self-gravitating state does not appear to be strictly determined by a maximum value of α . If the boundary was determined largely by a maximum expected value of α , it should lie along one of the solid contours in Fig. 6. The actual boundary is illustrated by the dashed-line in Fig. 6. As β decreases, the value of Q_{irr} required to halt fragmentation is larger than would be expected. The maximum quasi-steady α is also, consequently, smaller than expected. This suggests that the local cooling rate can influence fragmentation, although it appears that for every cooling time there is a Q_{irr} that inhibits fragmentation. We would expect that for sufficiently large Q_{irr} (e.g., vertical dash-dot line at $Q_{\text{irr}} = 1.95$ in Fig. 6) there would be no instability growth as the disc would be maintained above the threshold for linear instability. Also, for $Q_{\text{irr}} = 1.6$, fragmentation occurs for both $\beta = 4$ and $\beta = 5$, while for $Q_{\text{irr}} = 1.7$ a quasi-steady state is achieved for both values of β : this suggests that there may be a boundary region (i.e., between $Q_{\text{irr}} = 1.7$ and $Q_{\text{irr}} = 1.95$) in which a quasi-steady, self-gravitating state is achieved for all values of β . However, it is also possible that for sufficiently small values of β there could be no value of Q_{irr} for which a quasi-steady (i.e., self-gravitating but non-fragmenting) state is achieved. If so, the system would either undergo fragmentation or be linearly stable. This

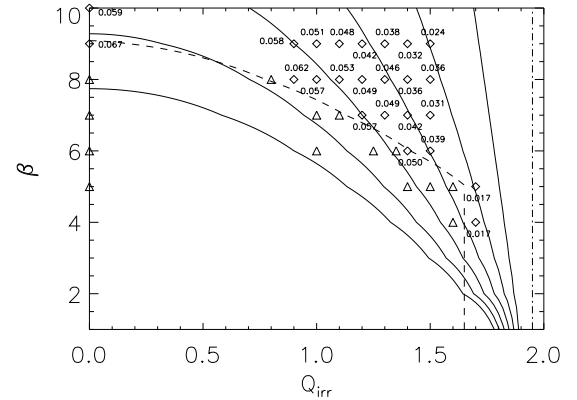


Figure 6. Figure showing contours of constant α determined using equation (15) with $Q_{\text{sat}} = 1.9$. The contour levels are $\alpha = 0.06, 0.05, 0.04, 0.03, 0.02$, and 0.01 . The symbols represent all the simulations, with the diamonds being those that settled into a quasi-steady state and the triangles being those that fragmented. The number next to each diamond is the measured α value for that simulation. The dashed line is the apparent boundary between fragmentation and a quasi-steady, self-gravitating state in the presence of irradiation. The dash-dot line illustrates the value of Q_{irr} above which we would expect systems to undergo no instability growth as they would be above the threshold for linear stability.

could have implications for mass loading of systems with very short cooling times. If there are indeed cooling times for which a quasi-steady state cannot exist then it suggests that such systems would be unable to viscously respond to increases in surface density and would typically go from being linearly stable to fragmenting if the surface density increases sufficiently. The long growth timescales of the instability in systems with large values of Q_{irr} is, however,

very long and so we don't attempt to determine here precisely what happens for very short cooling times.

Ultimately, we have been able to robustly determine the fragmentation properties of discs with $0 < Q_{\text{irr}} \leq 1.6$, reaching values at the top end that are close to the limit where irradiation entirely quenches gravitational instability. In this range, we find that irradiation modestly suppresses the critical value of β below which fragmentation occurs, from a value of $\beta_{\text{crit}} \approx 8$ in the absence of irradiation down to a value $\beta_{\text{crit}} \approx 4$ for the most strongly irradiated disc simulated. The maximum value of α that a self-gravitating disc can sustain similarly decreases as the strength of irradiation is increased.

Cossins, Lodato & Clarke (2009) suggests that there is a relationship between the perturbation amplitude ($\delta\Sigma/\Sigma$) and the cooling parameter, β . In particular they find that the rms averaged perturbation amplitude, $\langle\delta\Sigma/\Sigma_{\text{avg}}\rangle$, obeys the following relationship

$$\left\langle \frac{\delta\Sigma}{\Sigma_{\text{avg}}} \right\rangle \approx \frac{1.0}{\sqrt{\beta}}. \quad (16)$$

If, as suggested above, the fragmentation boundary is determined primarily by the effective α rather than by the imposed cooling, β , we might expect that the perturbation amplitude would depend on α rather than β . Fig. 7, shows α plotted against $\langle\delta\Sigma/\Sigma\rangle$ for all the simulations we performed that did not fragment. The diamonds are for all the simulations with $Q_{\text{irr}} = 0$ (i.e., Fig. 4) while the other symbols are for the simulations with $Q_{\text{irr}} \neq 0$ and correspond to the simulations illustrated in Fig. 5, although we have also added the $\beta = 4$, $\beta = 5$ and $\beta = 6$ simulations that aren't included in Fig. 5. The values for $\langle\delta\Sigma/\Sigma_{\text{avg}}\rangle$ were determined by averaging over at least 10 slices starting after the quasi-steady state was reached. The error bars are 1σ errors. The curve in Fig. 7 is $\alpha \propto (\langle\delta\Sigma/\Sigma\rangle)^2$ and is essentially equivalent to equation (16), taken from Cossins, Lodato & Clarke (2009). Fig. 7 therefore confirms that there is a relationship between the perturbation amplitude and the effective α , rather than the cooling time. That this holds for both irradiated and non-irradiated discs illustrates that it is universal and is essentially independent of the condition of thermal equilibrium.

The reason we have plotted α against $\langle\delta\Sigma/\Sigma\rangle$, rather than the other way around, is to highlight that the fundamental relationship is that the magnitude of the effective α depends only on the magnitude of the density perturbations. If, as one might expect, fragmentation requires non-linear density perturbations ($\langle\delta\Sigma/\Sigma\rangle \geq 1$) this then implies that the maximum α that can be supplied by a quasi-steady system (i.e., one that does not fragment) is $\alpha \sim 0.06$, consistent with earlier results (Gammie 2001; Rice et al. 2003a). However, as illustrated above, it appears that for short cooling times fragmentation can occur even if the expected α is less than 0.06 which suggests that large, localised perturbations in these systems can grow to form bound clumps even if the perturbation amplitude in the system as a whole is typically small.

To further illustrate the universality between α and the perturbation amplitudes, we plot, in Fig. 8, the power spectrum of the perturbations for 4 of the simulations. As in Gammie (2001) the x-axis is in units of $kL/(2\pi)$ and since the power spectra all peak at $kL/(2\pi) \sim 7$, this illustrates that most of the power comes from wavelengths smaller than $L/7$ (i.e., the shear stress come primarily from wavelengths significantly smaller than the model size). Fig. 8 also shows that the power spectra all have the same basic form with, as expected, the amplitude increasing with increasing α . Furthermore, the two simulations with the approximately the same α values (but different values for β and Q_{irr}) have almost identical

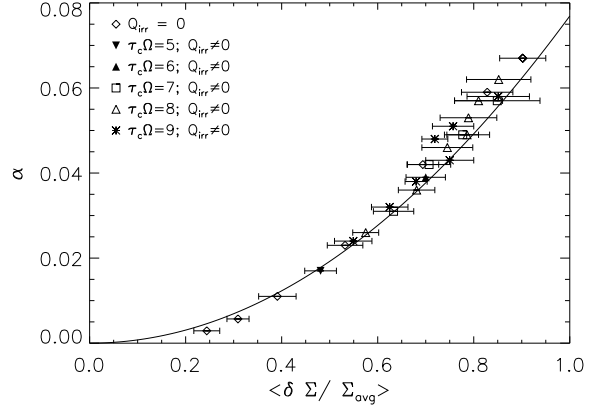


Figure 7. Figure showing the relationship between α and the rms averaged perturbation amplitude, $\langle\delta\Sigma/\Sigma\rangle$. The diamonds show the values for all the simulations with $Q_{\text{irr}} = 0$ while the others symbols represents the simulations with $Q_{\text{irr}} \neq 0$. The curve is $\alpha \propto (\langle\delta\Sigma/\Sigma\rangle)^2$ illustrating that there is a relationship between the perturbation amplitude and α irrespective of whether irradiation is present or not.

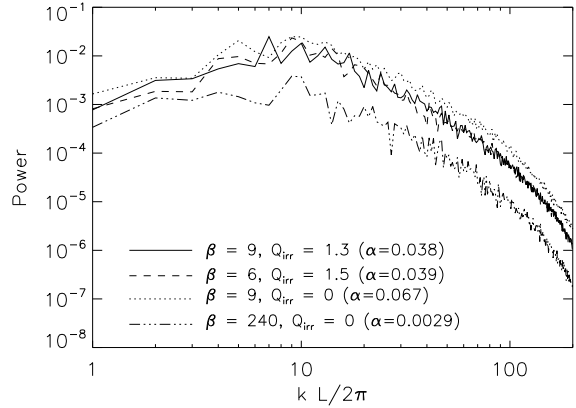


Figure 8. Power spectrum for 4 of the simulations. The x-axis is in units of $kL/(2\pi)$ so the peak at $kL/(2\pi) \sim 7$ illustrates that most of the shear stress comes from wavelengths significantly smaller than the model size. The power spectra all have the same basic structure with, as expected, the amplitude increasing with increasing α . The two simulations with approximately the same α values are almost identical illustrating that the structure of the turbulent state depends primarily on the effective value of α .

power spectra. This illustrates that the structure of the turbulent state does not depend on the cooling rate or the level of irradiation, but is determined only by the effective value of α .

4 CONCLUSIONS

For a self-gravitating accretion disc to fragment, gravitational instability must produce strong density perturbations that can cool quickly enough to collapse before shear and pressure forces disperse them. These requirements for fragmentation can be expressed via two dimensionless numbers: a maximum value of α , which fixes the amplitude of density fluctuations, and a minimum value of β , which measures the cooling time in terms of the local orbital

time scale. In the absence of external heating, local thermal equilibrium implies an exact equivalence between these descriptions, but this is no longer the case once irradiation becomes significant. In this paper, we have used local, two-dimensional simulations of self-gravitating discs to plot the fragmentation boundary in both isolated and irradiated discs. We find that the fragmentation boundary for irradiated discs does not lie at fixed values of either α or β . Irradiation necessarily weakens the strength of gravitational instability, but whether it stabilizes or destabilizes discs against fragmentation depends upon the chosen metric. In terms of the cooling time scale, irradiation stabilizes discs: a strongly irradiated disc can avoid fragmentation for cooling times almost a factor of two smaller than the limit for a non-irradiated disc. In terms of the maximum stress, however, irradiation has the opposite effect: the maximum α sustainable in an irradiated disc is lower than that reached in the absence of irradiation. This is somewhat counterintuitive but is likely a consequence of the universal nature of the form of the power spectrum of the perturbations. Although irradiation weakens the instability, it is still possible for large, local perturbations to exist. If the cooling time is sufficiently short then these large perturbations could collapse to form fragments even if the typical perturbations are small (i.e., $\alpha_{\text{eff}} < 0.06$).

For protoplanetary discs, the implication of our results is to reinforce the conclusion that the outer regions of protoplanetary discs are generally unstable to fragmentation at the high accretion rates encountered soon after disc formation (Clarke 2009; Cossins, Lodato & Clarke 2010). For a disc forming in a cold environment ($T \approx 10$ K), the rate of infall at radii $r \sim 50 - 100$ AU may well exceed the maximum accretion rate ($\dot{M} \sim 10^{-7} M_{\odot} \text{ yr}^{-1}$) that can be transported inward by the magnetorotational instability, even if the MRI is active at these radii despite the effects of ambipolar diffusion (Bai & Stone 2011). If so, continued infall will result in the build up of surface density until self-gravity sets in, at which point our results imply that irradiation will not save the disc from fragmentation. Irradiation will, of course, increase the surface density and temperature of the critically fragmenting disc, making it (even) more likely that the outcome of fragmentation will be substellar objects rather than massive planets (Rice et al. 2003b; Stamatellos, Hubber & Whitworth 2007). Discs forming in substantially warmer environments ($T \approx 100$ K) have a better chance of avoiding fragmentation, since the MRI in these systems may be able to transport all the infalling gas inward without locally exceeding the threshold surface density for gravitational instability. If all other aspects of star formation remained fixed, we would therefore expect to see more wide binaries in cool environments, and more young extended gas discs in warmer star forming climes.

Finally, we caution that our results strictly apply only to the stability of *isolated* self-gravitating discs. Protoplanetary discs approaching the threshold surface density for gravitational instability do so on account of infall, which need not be steady or axisymmetric. The dynamical effects of infall appear to stabilize discs against fragmentation (Kratter et al. 2010; Harsono, Alexander & Levin 2011), at least to some degree, but further work is needed to ascertain whether it is possible to avert fragmentation indefinitely at radii where isolated local disc models predict collapse.

ACKNOWLEDGMENTS

This work was started at the Dynamics of Discs and Planets programme at the Isaac Newton Institute for Mathematical Sciences, and we wish to thank both the organizers and the In-

stitute for their support. P.J.A. acknowledges support from the NSF (AST-0807471), from NASA's Origins of Solar Systems program (NNX09AB90G), and from NASA's Astrophysics Theory program (NNX11AE12G). GRM acknowledges support from the Scottish Universities Physics Alliance (SUPA) and WKMR from STFC grant ST/H002380/1. This work made use of the facilities of HECToR, the UK's national high-performance computing service, which is provided by UoE HPCx Ltd at the University of Edinburgh, Cray Inc and NAG Ltd, and funded by the Office of Science and Technology through EPSRC's High End Computing Programme. The authors would like to thank Anders Johansen for help with the Pencil Code and Charles Gammie, Kaitlin Kratter, and Ruth Murray-Clay for useful discussions.

REFERENCES

- Armitage P. J., 2011, *ARA&A*, 49, 195 (arXiv:1011.1496v2)
- Bai X.-N., & Stone J. M., 2011, *ApJ*, 736, 144
- Balbus S. A., & Papaloizou J. C. B., 1999, *ApJ*, 521, 650
- Boley A. C., 2009, *ApJ*, 695, L53
- Bonnell I. A., & Rice W. K. M., 2008, *Science*, 321, 1060
- Boss, A. P., 1997, *Science*, 276, 1836
- Brandenburg A., 2003, in *Advances in Nonlinear Dynamos*, ed. A. Ferriz-Mas & M. Núñez (London: Taylor & Francis), 269
- Cai K., Durisen R. H., Boley A. C., Pickett M. K., Mejia A. C., 2008, *ApJ*, 1138
- Clarke C. J., 2009, *MNRAS*, 396, 1066
- Cossins P., Lodato G., & Clarke C. J., 2009, *MNRAS*, 393, 1157
- Cossins P., Lodato G., & Clarke C. J., 2010, *MNRAS*, 401, 2587
- Gammie C. F., 2001, *ApJ*, 553, 174
- Goodman J., 2003, *MNRAS*, 339, 937
- Harsono D., Alexander R. D., & Levin Y., 2011, *MNRAS*, 413, 423
- Johnson B. M., & Gammie C. F., 2003, *ApJ*, 597, 131
- Kratter K. M., & Murray-Clay R., 2011, *ApJ*, in press (arXiv:1107.0728v1)
- Kratter K. M., Matzner C. D., Krumholz M. R., & Klein R. I., 2010, *ApJ*, 708, 1585
- Levin Y., 2007, *MNRAS*, 374, 515
- Lin D. N. C., & Pringle J. E., 1987, *MNRAS*, 225, 607
- Lin D. N. C., & Pringle J. E., 1990, *ApJ*, 358, 515
- Lodato G., & Clarke C. J., 2011, *MNRAS*, 413, 2735
- Lodato G., & Rice W. K. M., 2005, *MNRAS*, 351, 630
- Mamatsashvili G. R., & Rice W. K. M., 2010, *MNRAS*, 406, 2050
- Mamatsashvili G. R., & Rice W. K. M., 2009, *MNRAS*, 394, 2153
- Matzner C. D., & Levin Y., 2005, *ApJ*, 628, 817
- Meru F., & Bate M. R., 2011, *MNRAS*, 411, L1
- Paczynski B., 1978, *Acta Astronomica*, 28, 91
- Paardekooper S.-J., Baruteau C., & Meru F. 2011, *MNRAS*, in press (arXiv:1106.4425v1)
- Pringle J. E., 1981, *ARA&A*, 19, 137
- Rafikov R. R., 2005, *ApJ*, 631, L69
- Rafikov R. R., 2009, *ApJ*, 704, 281
- Rice W. K. M., Armitage P. J., Bate, M. R., & Bonnell, I. A., 2003, *MNRAS*, 339, 1025
- Rice W. K. M., Armitage P. J., Bonnell I. A., Bate M. R., Jeffers S. V., & Vine, S. G., 2003, *MNRAS*, 346, L36
- Rice W. K. M., Forgan D., & Armitage P. J., 2011, *MNRAS*, submitted
- Rice W. K. M., Lodato G., & Armitage P. J., 2005, *MNRAS*, 364, 56

- Rice W. K. M., Mayo J. H., & Armitage P. J., 2010, MNRAS, 402, 1740
Romeo A. B., 1992, MNRAS, 256, 307
Shakura N. I., & Sunyaev R. A., 1973, A&A, 24, 337
Shlosman I., & Begelman M. C., 1987, Nature, 329, 810
Stamatellos D., Hubber D. A., & Whitworth A. P., 2007, MNRAS, 382, L30
Toomre A., 1964, ApJ, 139, 1217